Electronic Supplementary Material (ESI) for Polymer Chemistry.

## Supporting Information for

# Limonene Induced Chiroptical Generation and Inversion during Aggregation of Achiral Polyfluorene Analogs: Structure-dependency and Mechanism

*Laibing Wang,*[a] *Nozomu Suzuki,*[b] *Jiangfei Liu,*[a] *Takashi Matsuda,*[b] *Nor Azura Abdul Rahim,*[b] *Wei Zhang,**[a] *Michiya Fujiki,**[b] *Zhengbiao Zhang,* [a] *Nianchen Zhou*[a] *and Xiulin Zhu*[a]

[a]Jiangsu Key Laboratory of Advanced Functional Polymer Design and Application, Department of Polymer Science and Engineering, College of Chemistry, Chemical Engineering and Materials Science, Soochow University, Suzhou Industrial Park, Suzhou 215123, China
[b]Graduate School of Materials Science, Nara Institute of Science and Technology, 8916-5 Takayama, Ikoma, Nara 630-0192, Japan

## Experimental Section

**Materials.** Tetrakis(triphenylphosphine)-palladium(0) (97.0%, TCI), 2,7-dibromo-9,9-di-*n*-octylfluorene (98.0%, Tokyo Chemical Industry (TCI), Tokyo, Japan), 9,9-dioctylfluorene-2,7-diboronic acid (98.0%, J&K Scientific (Beijing, China)), 2,7-bis(4,4-5,5-tetramethyl-1,3,2-dioxaborolan-2-yl)-9,9-dioctylsilafluorene, 2,7-dibromo-9,9-dioctylsilafluorene, 9-(1-octylnonyl) carbazole-2,7-bis(boronic acid pinacol ester) and 2,7-dibromo-9-(1-octylnonyl)-9*H*-carbazole (98.0%, Derthon Optoelectronic Materials Sci. and Tech. (Shenzhen, China)) were used as received. (*R*)-Limonene (**1*R***) and (*S*)-limonene (**1*S***) were obtained from TCI and were distilled at reduced pressure prior to use. Optical rotation (24 °C, neat liquid, 1.0 cm path length, synthetic (SQ) cuvette, Na-d line) obtained with JASCO, P-1020 polarimeter showed that, unpurified **1*R*** and **1*S*** had $[\alpha]^{24}{}_{589}$ = +99.62° and -97.72°, respectively, and distilled **1*R*** and **1*S*** were $[\alpha]^{24}{}_{589}$ = +102.29° and -98.29°, respectively. The solvents used in the optical properties here were purified by reduced distillation before use. All the other chemicals were obtained from Shanghai Chemical Reagents (Shanghai, China) and used as received. Three homopolymers (**PF8**, **PSi8**, and **PCz8**), three alternating copolymers **(P(F8-*alt*-Si8)**, **P(F8-*alt*-Cz8)**, **P(Si8-*alt*-Cz8))**, and one random copolymer **P(F8$_{0.80}$-*ran*-PSi8$_{0.20}$)** were synthesized by the SPC as described in Scheme S1. The full synthetic procedures, and weight-average and number-average molecular weights ($M_w$ and $M_n$) and molecular weight distributions ($M_w/M_n$) measured by gel permeation chromatography (GPC) (Fig. S1) were presented as following.

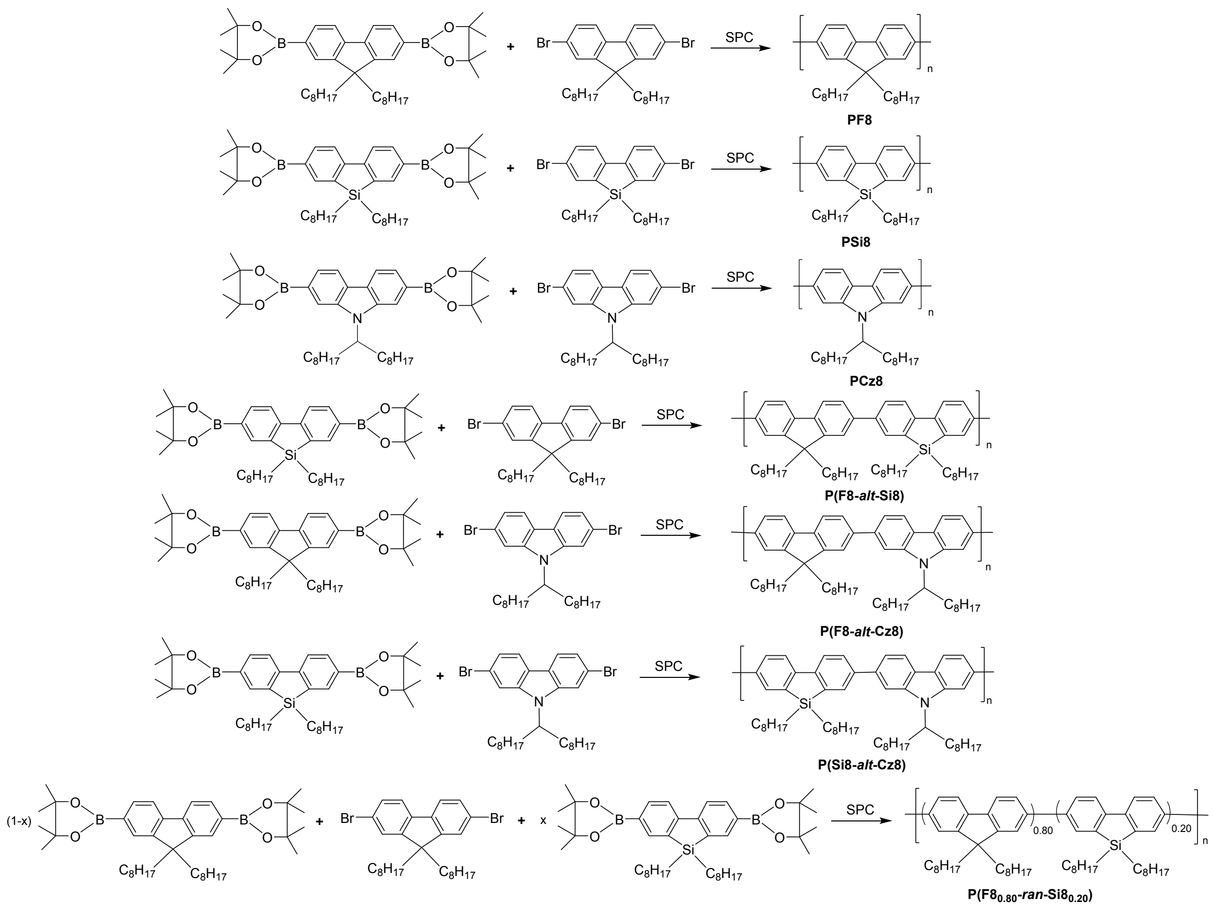

**Scheme S1.** The synthetic routes of π-conjugated polymers used in this study.

## Synthesis of *π*-conjugated polymers

As shown in Scheme S1, all the polymers were synthesized using Suzuki coupling (SPC) reaction. Taking the synthesis of **PSi8** as an example: 2,7-bis(4,4-5,5-tetramethyl-1,3,2-dioxaborolan-2-yl)-9,9-dioctylsilafluorene (581 mg, 0.883 mmol), 2,7-dibromo-9,9-dioctyl-silafluorene (500 mg, 0.883 mmol) and $Pd(PPh_3)_4$ (0) (10.2 mg, 0.00883 mmol) were dissolved in a mixture of THF (4.5 mL) and 2 M $Na_2CO_3$ (3.0 mL) under nitrogen atmosphere. The solution was vigorously stirred at 80 °C for 72 h. The whole mixture was poured into a mixture of methanol and water (500 mL, $CH_3OH/H_2O$ = 10/1 (v/v)). The precipitate was obtained by filtration and washed with a large amount of water. The resulting precipitate was washed for 72 h in a Soxhlet extracting apparatus using acetone to remove oligomers and catalyst residues. The resulting polymer produced an off-white solid (0.692g, 64.1%). $M_n$ = 14050 g mol$^{-1}$, $M_w/M_n$ = 2.38. $(C_{28}H_{42}Si)_n$ $(406.7)_n$: Calcd. C 82.69, H 10.41; Found C 79.38, H 9.97. $^1$H NMR (400 MHz, $CDCl_3$): δ (ppm) 0.50-1.75 (brm, $CH_2$+$CH_3$), 6.30-7.00 (brm, Ar*H*), 7.40-8.25 (brm, Ar*H*).

**PF8** was synthesized using a similar procedure to **PSi8**. 2,7-dibromo-9,9-di-*n*-octylfluorene (200 mg, 0.311mmol) and 9,9-dioctylfluorene-2,7-diboronic acid (170.70 mg, 0.311 mmol) took the place of 2,7-dibromo-9,9-dioctylsilafluorene and 2,7-bis(4,4-5,5-tetramethyl- 1,3,2-dioxaborolan-2-yl)-9,9-dioctylsilafluorene, respectively. The resulting polymer produced a yellowish green solid powder (0.198 g, 53.5% yield). $M_n$ = 48230 g mol$^{-1}$, $M_w/M_n$ = 2.75. $(C_{29}H_{42})_n$ $(390.3)_n$: Calcd. C 89.16, H 10.84; Found C 86.92, H 10.32. $^1$H NMR (400 MHz, $CDCl_3$): δ (ppm) 0.50-1.75 (brm, $CH_2$+$CH_3$), 2.33-1.89 (brm, $CH_2$), 7.50-8.10 (brm, Ar*H*).

**PCz8** was also synthesized by a procedure similar to **PSi8**. 2,7-dibromo-9-(1- octylnonyl)-9H-carbazole (257.00 mg, 0.382 mmol) and 9-(1-octylnonyl) carbazole-2,7-bis (boronic acid pinacol ester) (215.00 mg, 0.382 mmol) took the place of 2,7-dibromo-9,9-dioctylsilafluorene and 2,7-bis(4,4-5,5-tetramethyl-1,3,2-dioxaborolan- 2-yl)-9,9-dioctylsilafluorene, respectively. The resulting polymer produced a light yellow fibrous solid (0.281 g, 59.6% yield). $M_n$ = 85390 g mol$^{-1}$, $M_w/M_n$ = 3.02. $(C_{29}H_{43}N)_n$ $(405.3)_n$: Calcd. C 85.86, H 10.68, N 3.45; Found C 82.85, H 10.36, N 3.35. $^1$H NMR (400 MHz, $CDCl_3$): δ (ppm) 0.72-0.90 (brm, $CH_3$), 1.06-1.45 (brm, $CH_2$), 1.94-2.18 (brm, $CH_2$), 2.35-2.61 (brm, $CH_2$), 4.60-4.93 (brm, CH), 7.53-8.03 (brm, Ar*H*), 8.13-8.40 (brm, Ar*H*).

**P(F8-*alt*-Si8)** was synthesized by a similar procedure to **PSi8**. 2,7-dibromo-9,9-di- *n*-octylfluorene (170.70 mg, 0.311 mmol) to the place of 2,7-dibromo-9,9-di-*n*-octylsilafluorene and 2,7-bis(4,4-5,5-tetramethyl-1,3,2-dioxaborolan-2-yl)-9,9-di-*n*-octylsila-fluorene (240.70 mg, 0.311 mmol) was remained. The resulting polymer produced a grey green flake solid (0.223 g, 54.2% yield). $M_n$ = 32770 g mol$^{-1}$, $M_w/M_n$ = 2.58. $(C_{57}H_{82}Si)_n$ $(794.6)_n$: Calcd. C 86.08, H 10.39; Found C 80.31, H 9.68. $^1$H NMR (400 MHz, $CDCl_3$): δ (ppm) 0.60-0.93 (brm, $CH_2$), 0.94-1.43 (brm, $CH_2$+$CH_3$), 1.88-2.51 (brm, $CH_2$), 7.40-8.28 (brm, Ar*H*).

**P(F8$_{0.80}$-*ran*-Si8$_{0.20}$)** was synthesized by a similar procedure with **PSi8**. 2,7-bis(4,4-5,5-tetramethyl-1,3,2-dioxaborolan-2-yl)-9,9-di-*n*-octylsilafluorene (98.80 mg, 0.150 mmol), 2,7-bis(4,4-5,5-tetramethyl-1,3,2-dioxaborolan-2-yl)-9,9-di-*n*-octylfluorene (96.40 mg, 0.150

mmol), 2,7-dibromo-9,9-di-*n*-octylsilafluorene (164.50 mg, 0.300 mmol) and $(PPh_3)_4Pd(0)$ (3.60 mg, 0.00150 mmol) were dissolved in a mixture of THF (3.0 mL) and 2 M $Na_2CO_3$ (2.0 mL) under nitrogen atmosphere. The resulting polymer produced a grey green flake solid with 51.4% yield. The relative ratio of F8 and Si8 units in the final polymer chain was calculated based on the corresponding integrals at δ = 1.95-2.41 and δ = 7.45-8.35, which were attributed to the methylene protons close to 9-position carbon atom and the protons of aromatic rings, respectively. $M_n = 31500$ g·mol$^{-1}$, $M_w/M_n = 3.77$. Anal. Calcd. for $(C_{28.8}H_{42}Si_{0.2})n$ (393.8)n: C 87.81; H 10.77 %. Found: C 81.92; H 9.77 %. $^1$H NMR (400 MHz, $CDCl_3$): δ (ppm) 0.60-0.95 (brm, $CH_2$+$CH_3$), 0.97-1.45 (brm, $CH_2$+$CH_3$), 1.95-2.41 (brm, $CH_2$), 7.45-8.35 (brm, Ar*H*).

**P(F8-*alt*-Cz8)** was synthesized by a similar procedure as **PSi8**. 2,7-dibromo-9,9-di- *n*-octylfluorene and 9-(1-octylnonyl) carbazole-2,7-bis(boronic acid pinacol ester) took the place of 2,7-dibromo-9,9-dioctylsilafluorene and 2,7-bis(4,4-5,5-tetramethyl-1,3,2-dioxaborolan-2-yl)-9,9-dioctylsilafluorene respectively. The resulting polymer produced a light yellow fibrous solid (yield: 48.5%). $M_n = 87400$ g mol$^{-1}$, $M_w/M_n = 3.31$. $(C_{58}H_{83}N)_n$ $(793.6)_n$: Calcd. C 87.70, H 10.53, N 1.76; Found C 84.11, H 10.39, N 1.88. $^1$H NMR (400 MHz, $CDCl_3$): δ (ppm) 0.70-0.96 (brm, $CH_2$+$CH_3$), 1.02-1.46 (brm, $CH_2$+$CH_3$), 4.59-5.01 (brm, C*H*), 7.44-8.08 (brm, Ar*H*), 8.13-8.50 (brm, Ar*H*).

**P(Si8-*alt*-Cz8)** was synthesized by the similar procedure as **PSi8**. 2,7-dibromo-9,9-dioctylsilafluorene and 9-(1-octylnonyl) carbazole-2,7-bis(boronic acid pinacol ester) took the place of 2,7-dibromo-9,9-dioctylsilafluorene and 2,7-bis(4,4-5,5-tetramethyl-1,3,2-dioxa-borolan-2-yl)-9,9-dioctylsilafluorene and 2,7-bis(4,4-5,5-tetramethyl-1,3,2-dioxaborolan-2- yl)-9,9-dioctylsilafluorene, respectively. The resulting polymer produced a light yellow flake solid (yield: 47.4%). $M_n = 72470$ g mol$^{-1}$, $M_w/M_n = 4.34$. $(C_{57}H_{83}NSi)_n$ $(809.6)_n$ : Calcd. C 84.48, H 10.32, N 1.73; Found C 75.68, H 9.21, N 1.35. $^1$H NMR (400 MHz, $CDCl_3$): δ (ppm) 0.65-0.92 (brm, $CH_2$+$CH_3$), 0.94-1.44 (brm, $CH_2$+$CH_3$), 1.89-2.14 (brm, $CH_2$), 2.29-2.58 (brm, $CH_2$), 4.57-4.90 (brm, C*H*), 7.42-8.40 (brm, Ar*H*).

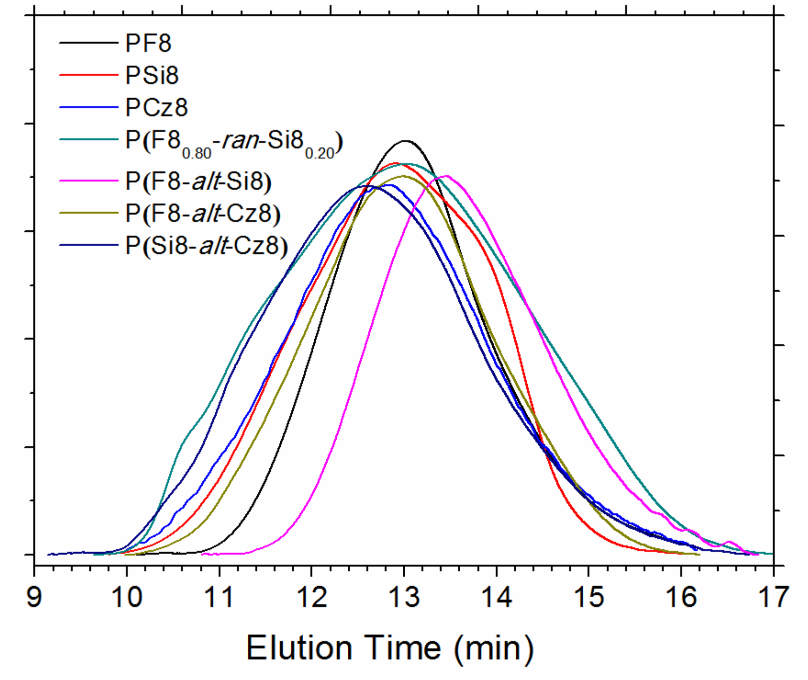

**Fig. S1** GPC curves of π-conjugated polymers.

**Preparation of π-Conjugated Polymer Aggregates.** Taking the preparation of **PSi8** aggregates as an example: the typical procedure for the production of **PSi8** aggregates in a mixed chloroform/limonene/methanol can be described as follows. First, 1.2 mL of **1*R*** or **1*S*** was added to 0.3 mL of a chloroform stock solution containing **PSi8** ([repeating unit]$_0$ = 5.0 × $10^{-5}$ mol $L^{-1}$) in synthetic quartz-grade (SQ)-cuvette, which was placed in the Peltier apparatus of a JASCO J-815 spectropolarimeter at 25 °C and stirred clockwise for 30 s at 1000 rpm. The addition of 1.5 mL methanol to the above solution at 25 °C resulted in an off-white turbid solution of **PSi8** aggregates dispersed in mixed solvents. After being stirred for 120 s, this solution was used for CD/UV-vis and fluorescent spectroscopic measurements. Other polymer aggregates in mixed solvents were obtained in a similar way.

**Gaussian03/09 Calculation.** All calculations were carried out using Gaussian03 (rev. E) and Gaussian09 (rev. D.01) running on an Apple PowerMac (dual QuadCore, 2.8 GHz, 32GB memory, MacOS ver.10.5.8, 2 TB hard disk). To predict the most probable structures, dipole moments, and Mulliken charges of **PF8**, **PSi8**, and **PCz8** in the ground state, the corresponding 9,9-di-*n*-octylfluorene (**F8**), 9,9-di-*n*-octylsilafluorene (**Si8**), and *N*-*n*-octyl-carbazole (**Cz8**) in (Scheme 2) were used with DFT (B3LYP/6-31G(d)) calculation. All **F8**,

**Si8**, and **Cz8** were assumed that *n*-octyl chain(s) adopt *trans-zigzag* structure that is vertical to the fluorene and silafluorene rings, whereas *n*-octyl chain of **Cz8** is oriented at in-plane of carbazole ring.

We used 9,9-dimethylfluorene trimer (**TriF1**), 9,9-dimethylsilafluorene trimer (**TriSi1**), and *N*-methylcarbazole trimer (**TriCz1**) (Scheme 2) with dihedral angles of +30° and +150° as model structures to simulate UV-vis and CD spectra of **PF8**, **PSi8**, and **PCz8**. Each repeat unit was optimized using DFT with B3LYP/6-31G(d,p) basis set and the dihedral angles of +30° and +150° corresponded to global and local minimum, respectively. Time-dependent density functional theory (TD-DFT with B3LYP/6-31G(d,p) basis set) was used for the energy calculation. To discuss possible interaction between **1*R*** and **PF8**/**PSi8**/**PCz8**, we obtained the dipole moments and Mulliken charges for the most probable, three equatorial rotamers of **1*R*** optimizing with DFT (B3LYP/6-31G(d,p) level) method. Mulliken charges of **PF8**, **PSi8** and **PCz8** in the excited state were obtained with configuration interaction singles (CIS) with 6-31G(d,p) basis set. Simulated UV and CD spectra of these three conformers were obtained with TD-DFT (B3LYP/6-31G(d,p) calculation.

**Characterization.** The number-average molecular weight ($M_n$) and molecular weight distribution ($M_w/M_n$) of the polymers were determined using a Waters 1515 gel permeation chromatograph (GPC) equipped with a refractive-index detector (Waters 2412), using HR1 (pore size: 100 Å, 100-5000 Da), HR2 (pore size: 500 Å, 500-20 000 Da), and HR4 (pore size 10 000 Å, 50-100 000 Da) columns (7.8 × 300 mm, 5 $\mu$m beads size) with molecular weights ranging from $10^2 \sim 5 \times 10^5$ g mol$^{-1}$. THF was used as the eluent at a flow rate of 1.0 mL min$^{-1}$ and 40 °C. GPC samples were injected using a Waters 717 plus autosampler and calibrated with polystyrene standards purchased from Waters. The $^1$H NMR spectra of the obtained polymer were recorded on an INOVA 400 MHz nuclear magnetic resonance (NMR) instrument (Agilent Technologies, Co, Ltd., Beijing, China) using $CDCl_3$ as the solvent and tetramethylsilane (TMS) as an internal standard. The elemental analysis was performed on a Vario EL elemental analysis instrument (Elementar Far East, Shanghai, China). The CD spectra were recorded at 25 °C on a JASCO J-815 spectropolarimeter (JASCO China, Shanghai, China) equipped with a Peltier-controlled housing unit using the SQ-grade cuvette, with a path length of 10 mm (with a scanning rate of 100 nm min$^{-1}$, a bandwidth of 2 nm and a response time of 1 s, using a single accumulation). The UV-vis spectra were simultaneously recorded on a Shimadzu UV-3150 spectrophotometer (Shimadzu China, Shanghai, China). Fluorescent spectra were measured on a PerkinElmer LS-50B spectrofluorometer (a scanning rate of 100 nm min$^{-1}$, an excitation bandwidth of 2 nm, a monitoring bandwidth of 2 nm, a response time of 1 s, 350 nm as excitation wavelength) at 25 °C. The CPL/PL spectra were recorded at 25 °C using a JASCO CPL-200 spectrofluoropolarimeter equipped with a Peltier-controlled housing and the SQ-grade quartz cuvette. A path length of 10 mm, a scanning rate of 100 nm min$^{-1}$, a bandwidth for excitation of 10 nm, a bandwidth for monitoring of 10 nm, a response time of 2 s, a 360 nm-excitation wavelength and single accumulation were employed. The size of the aggregates were measured by dynamic light scattering (DLS) using Malvern Zetasizer Nano-ZS90 at 25 °C at a scattering angle of 90°. The solution for the DLS measurement was used without any filtration. Fluorescence optical microscope (FOM) images were obtained as jpeg data using Nikon Eclipse E400 equipped with a mercury arc-discharge lamp and a filter block set UV1A. This block consists of a narrow band path filter for excitation at 360–370 nm, a long path dichroic mirror with >380 nm and a barrier filter with 420 nm as cut-on wavelength. For visibility, all original images were edited by a minimal image processing using auto-correction mode of iPhoto that is Apple MacOS10.75 built-in software.

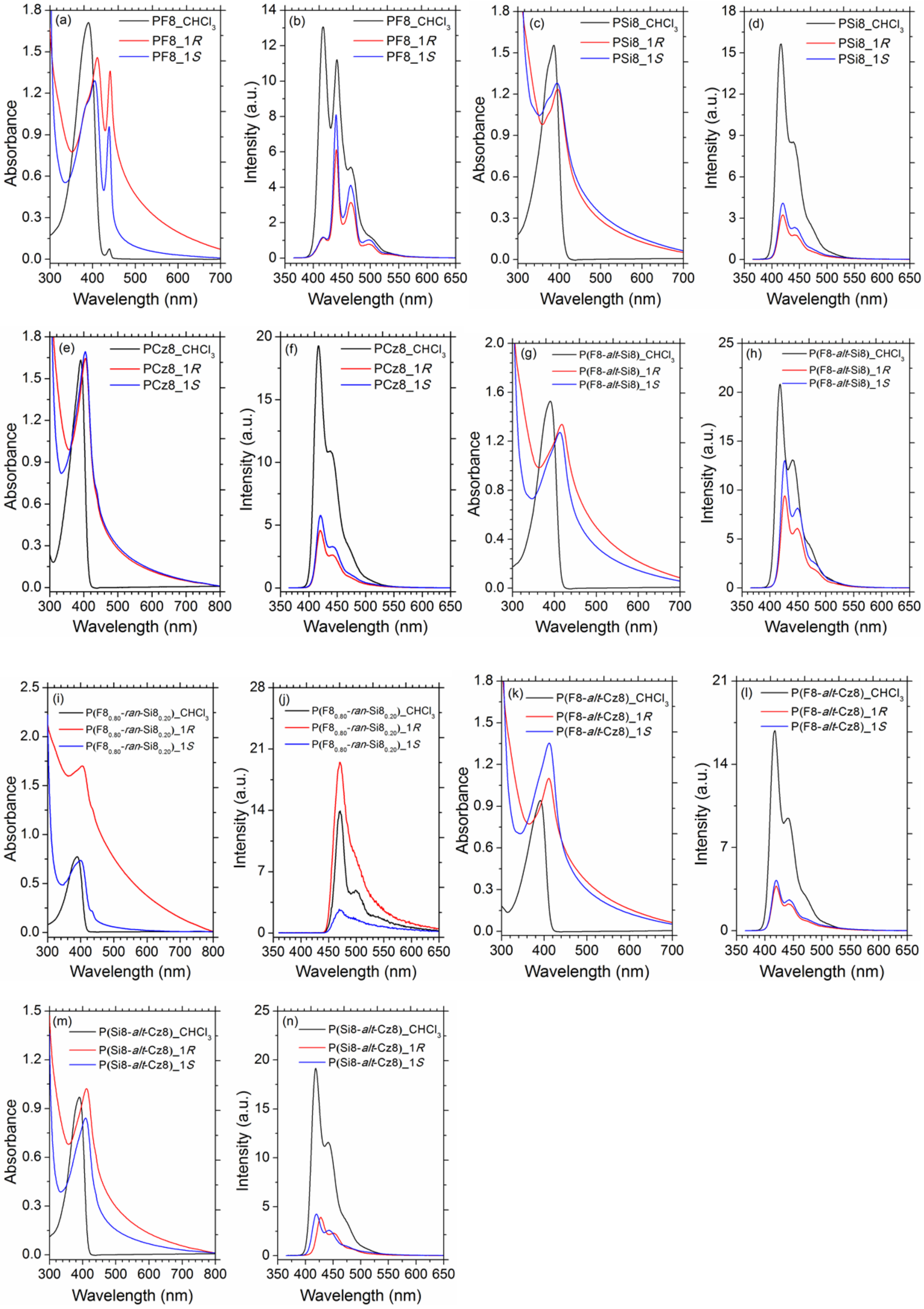

**Fig. S2** UV-vis and PL spectra of **PF8** (2a, 2b), **PSi8** (2c, 2d), **PCz8** (2e, 2f), **P(F8-*alt*-Si8)** (2g, 2h), **P(F8$_{0.80}$-*ran*-Si8$_{0.20}$)** (2i, 2j), **P(F8-*alt*-Cz8)** (2k, 2l), **P(Si8-*alt*-Cz8)** (2m, 2n) in $CHCl_3$ and $CHCl_3$/**1*R*** or **1*S***/$CH_3OH$ (0.3/1.2/1.5 for **PF8 PSi8** and **PCz8**, 0.3/0.8/1.9 for **P(F8-*alt*-Si8)**, **P(F8$_{0.80}$-*ran*-Si8$_{0.20}$)**, **P(F8-*alt*-Cz8)** and **P(Si8-*alt*-Cz8)**, v/v/v) at 25 °C. Conditions: **PF8** (1.94 × $10^{-2}$ mg mL$^{-1}$), **PSi8** and **PCz8** (1.41 × $10^{-2}$ mg mL$^{-1}$), **P(F8-*alt*-Si8)**, **P(F8$_{0.80}$-*ran*-Si8$_{0.20}$)**, and **P(F8-*alt*-Cz8)** (1.58 × $10^{-2}$ mg mL$^{-1}$), and **P(Si8-*alt*-Cz8)** (8.08 × $10^{-3}$ mg mL$^{-1}$).

As shown in Figs. S2g-2j, the very weak $\beta$-phase at ≈435 nm of **P(F8$_{0.80}$-*ran*-Si8$_{0.20}$)** aggregate was detected, but disappeared for **P(F8-*alt*-Si8)** aggregate in the same condition. Even in pure chloroform, **PF8** showed weak $\beta$-phase absorption at ≈435 nm (Fig. S2a), which was not the case for both **P(F8-*alt*-Si8)** (Fig. S2g) and **P(F8$_{0.80}$-*ran*-Si8$_{0.20}$)** (Fig. S2i). The above results indicate that the relative **Si8** contents of the polymer chain and aggregation states play a very important role to suppress the $\beta$-phase and show $\alpha$-phase only. In $CHCl_3$/**1*R***/$CH_3OH$, the CD signal changed steeply from negative value to a positive one with the increase of **Si8** contents in the polymer chain, and vice versa (Figs. 1a and S4).

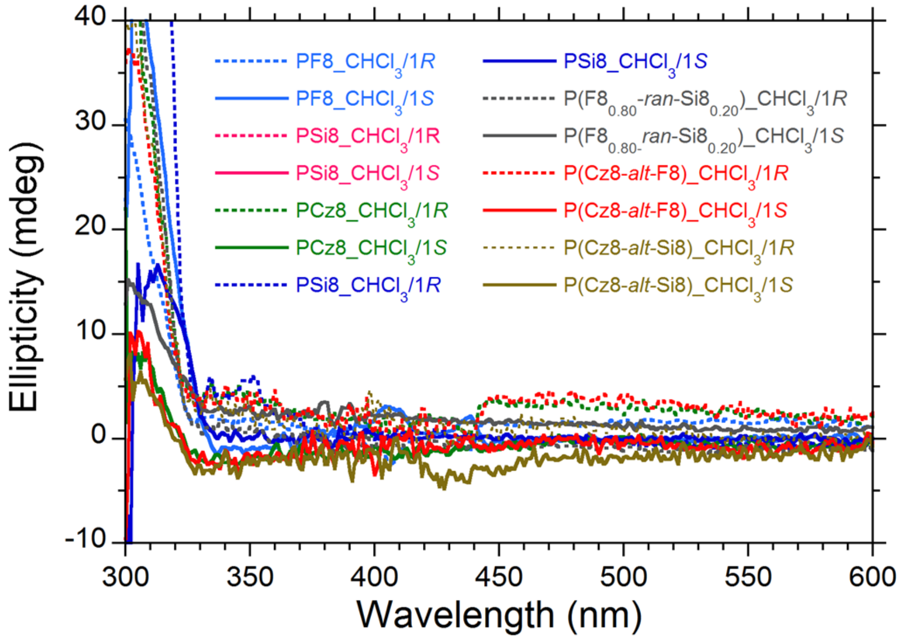

**Fig. S3** CD spectra of all the polymers in $CHCl_3$/(**1*R*** or **1*S***) (0.3/2.7, v/v). The concentrations of the polymers: **PF8** ($1.94 \times 10^{-2}$ mg mL$^{-1}$), **PSi8** and **PCz8** ($2.02 \times 10^{-2}$ mg mL$^{-1}$), **P(F8-*alt*-Si8)**, **P(F8$_{0.80}$-*ran*-Si8$_{0.20}$)**, and **P(F8-*alt*-Cz8)** ($1.98 \times 10^{-2}$ mg mL$^{-1}$), **P(Si8-*alt*-Cz8)** ($2.02 \times 10^{-2}$ mg mL$^{-1}$).

**Table S1.** The average particle size ($D_h$) and its distribution (PDI) of optically active $\pi$-conjugated polymers aggregates formed in the same conditions with the Fig. S2 at 25 °C.

| **Entry** | | **PF8** | **PSi8** | **PCz8** | **P(F8-*alt*-Si8)** | **P(F8$_{0.80}$-*ran*-Si8$_{0.20}$)** | **P(F8-*alt*-Cz8)** | **P(Si8-*alt*-Cz8)** |
|---|---|---|---|---|---|---|---|---|
| **$D_h$ (nm)** | **(*R*)** | 802.0 | 751.5 | 818.3 | 738.3 | 1029 | 725.7 | 647.2 |
| | **(*S*)** | 870.3 | 791.4 | 929.8 | 613.7 | 410.0 | 574.0 | 608.8 |
| **PDI** | **(*R*)** | 0.400 | 0.140 | 0.139 | 0.040 | 0.161 | 0.163 | 0.157 |
| | **(*S*)** | 0.336 | 0.101 | 0.197 | 0.056 | 0.170 | 0.105 | 0.130 |

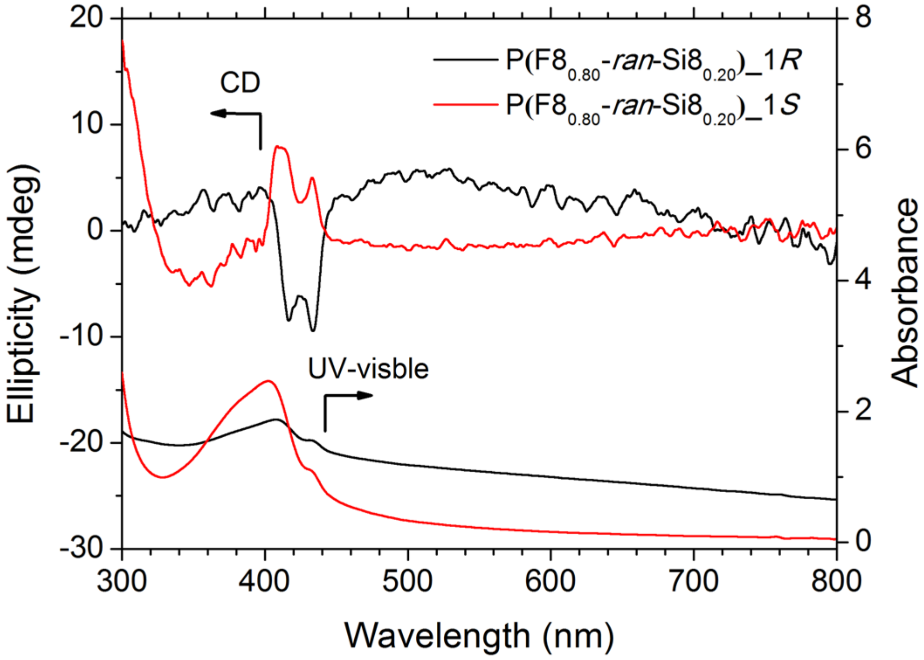

**Fig. S4** CD and UV-vis spectra of **P(F8$_{0.80}$-*ran*-Si8$_{0.20}$)** at 25 °C in CHCl$_3$/**1*R*** or **1*S***/CH$_3$OH (v/v/v) = 0.3/0.8/1.9 with a concentration of 1.98 × $10^{-2}$ mg mL$^{-1}$.

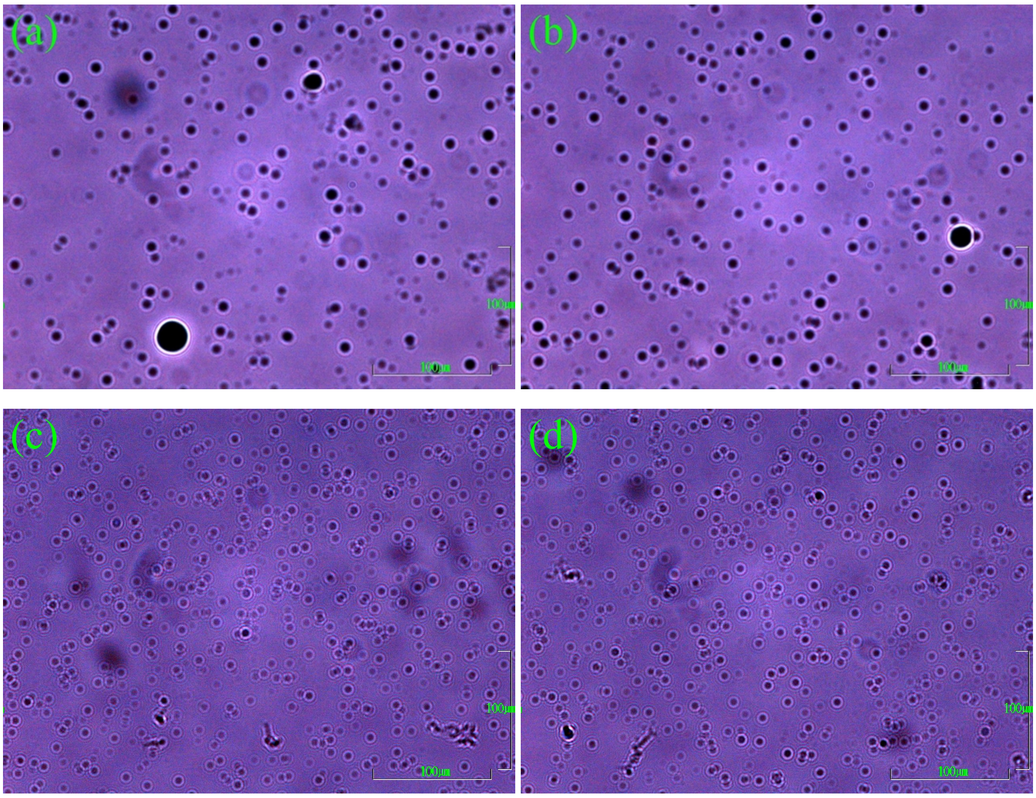

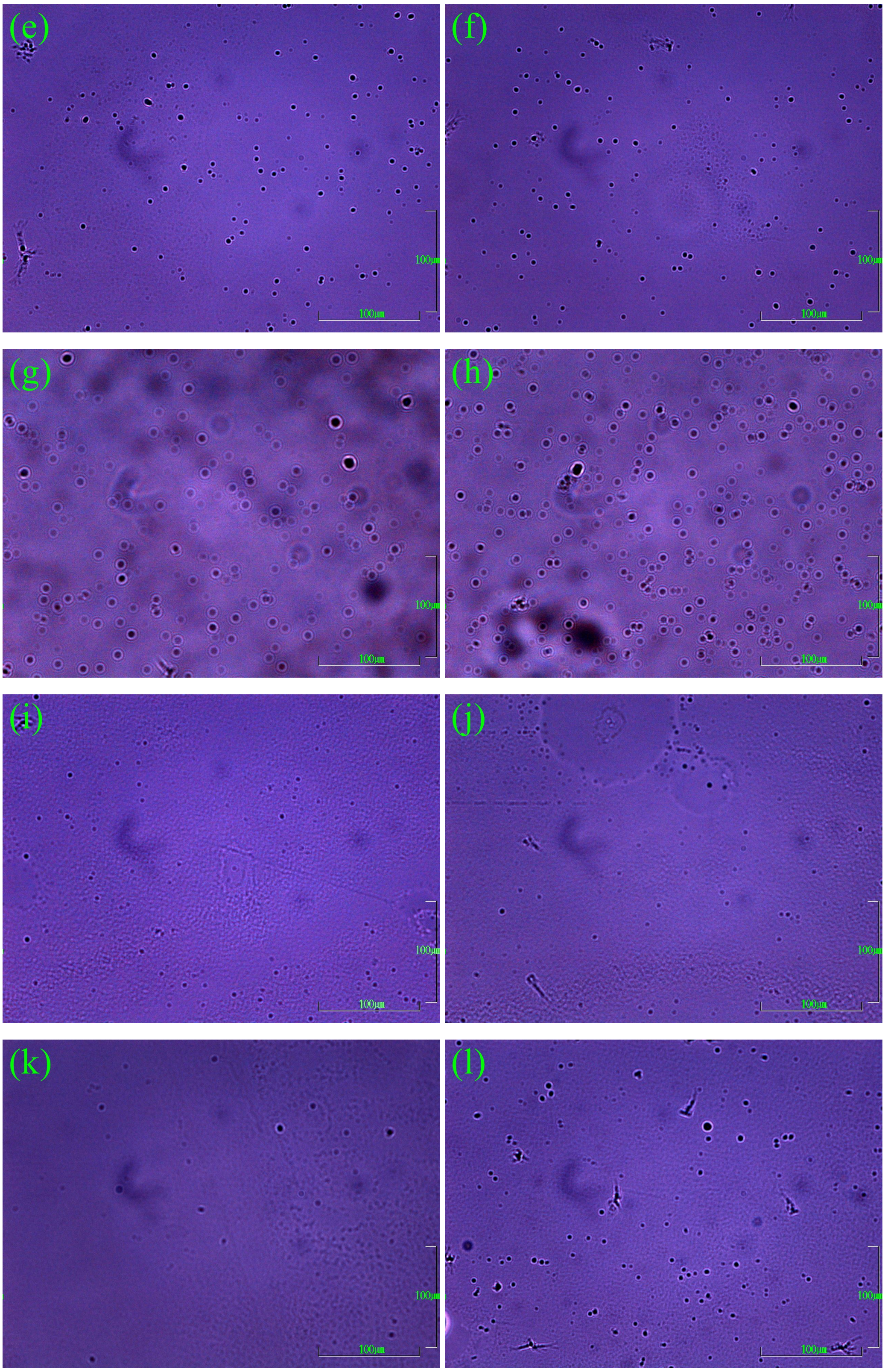

**Fig. S5** Fluorescence optical micrograph of microsphere due to polymers aggregates formed in the same conditions with the **Fig. S2** at 25 ˚C excited at 365 nm. **PF8** (**1*R*** (a) and **1*S*** (b)), **PSi8** (**1*R*** (c) and **1*S*** (d)), **PCz8** (**1*R*** (e) and **1*S*** (f)), **P(F8-*alt*-Si8)** (**1*R*** (g) and **1*S*** (h)), **P(F8-*alt*-Cz8)** (**1*R*** (i) and **1*S*** (j)), **P(Si8-*alt*-Cz8)** (**1*R*** (k) and **1*S*** (l)).

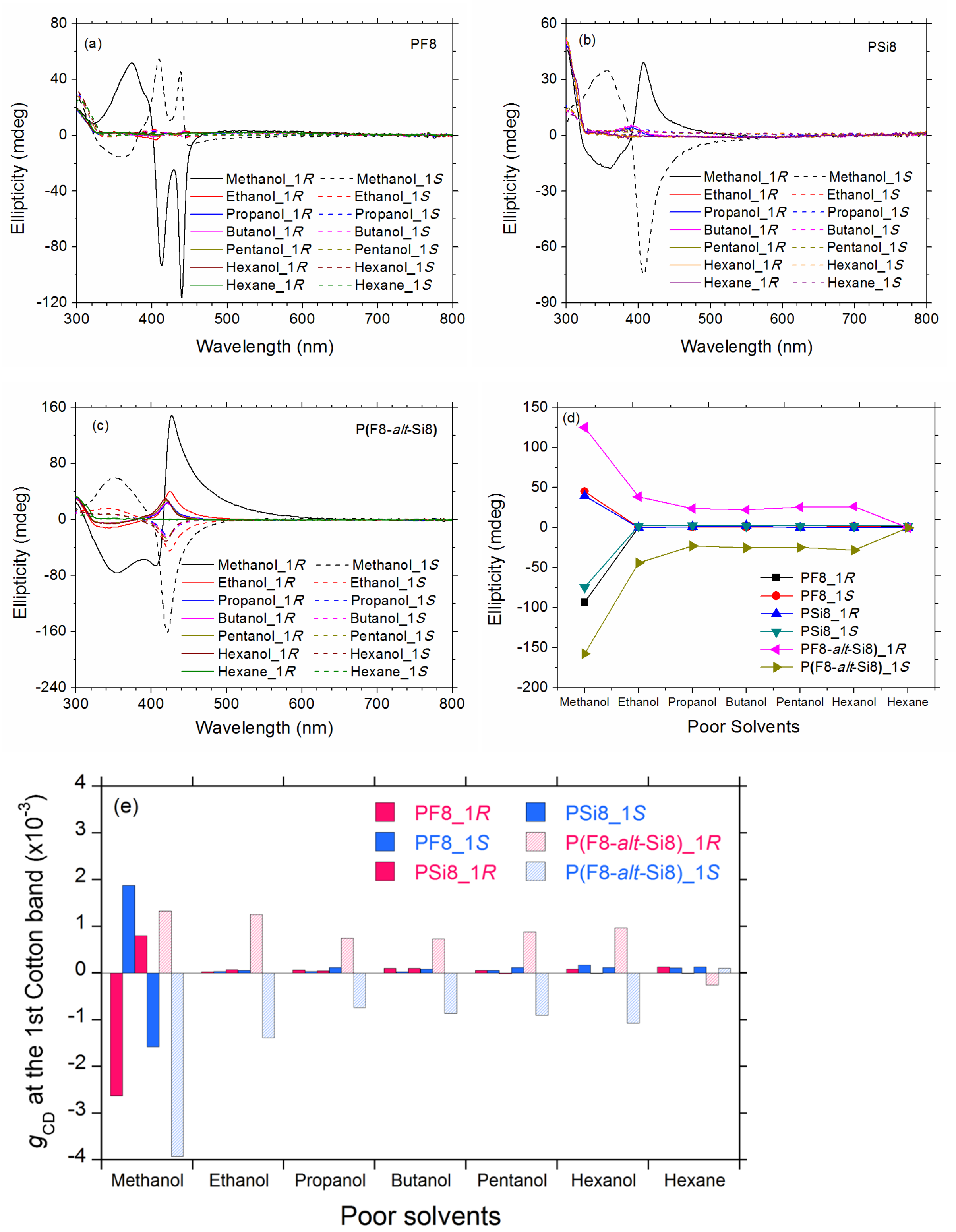

**Fig. S6** Chiroptical properties of homo- and co-polymer aggregates at 25 °C. CHCl$_3$/**1*R*** or **1*S***/poor solvent = 0.3/1.2/1.5 (v/v/v), 0.3/0.8/1.9, and 0.3/0.8/1.9 for **PF8**, **PSi8** and **P(F8-*alt*-Si8)**. The concentrations of the polymers are the same as those in Fig. 1a. (a) CD spectra of **PF8**. (b) CD spectra of **PSi8.** (c) CD spectra of **P(F8-*alt*-Si8)**. (d) The maximum CD values depending on poor solvent. The wavelength is 413 nm for **PF8**, 407 nm for **PSi8**, and 423 nm for **P(F8-*alt*-Si8)**. The data were taken from Figs. S6a-c. (e) the $g_{CD}$ values of homo- and copolymer aggregates with different poor solvents at 25 °C. The order of the a bar chart in each solvent are **PF8** with **1*R***, **1*S***, **PSi8**, with **1*R***, **1*S***, **P(F8-*alt*-Si8)** with **1*R*** and **1*S*** from left to right. The data were taken from Figs. S6a-c.

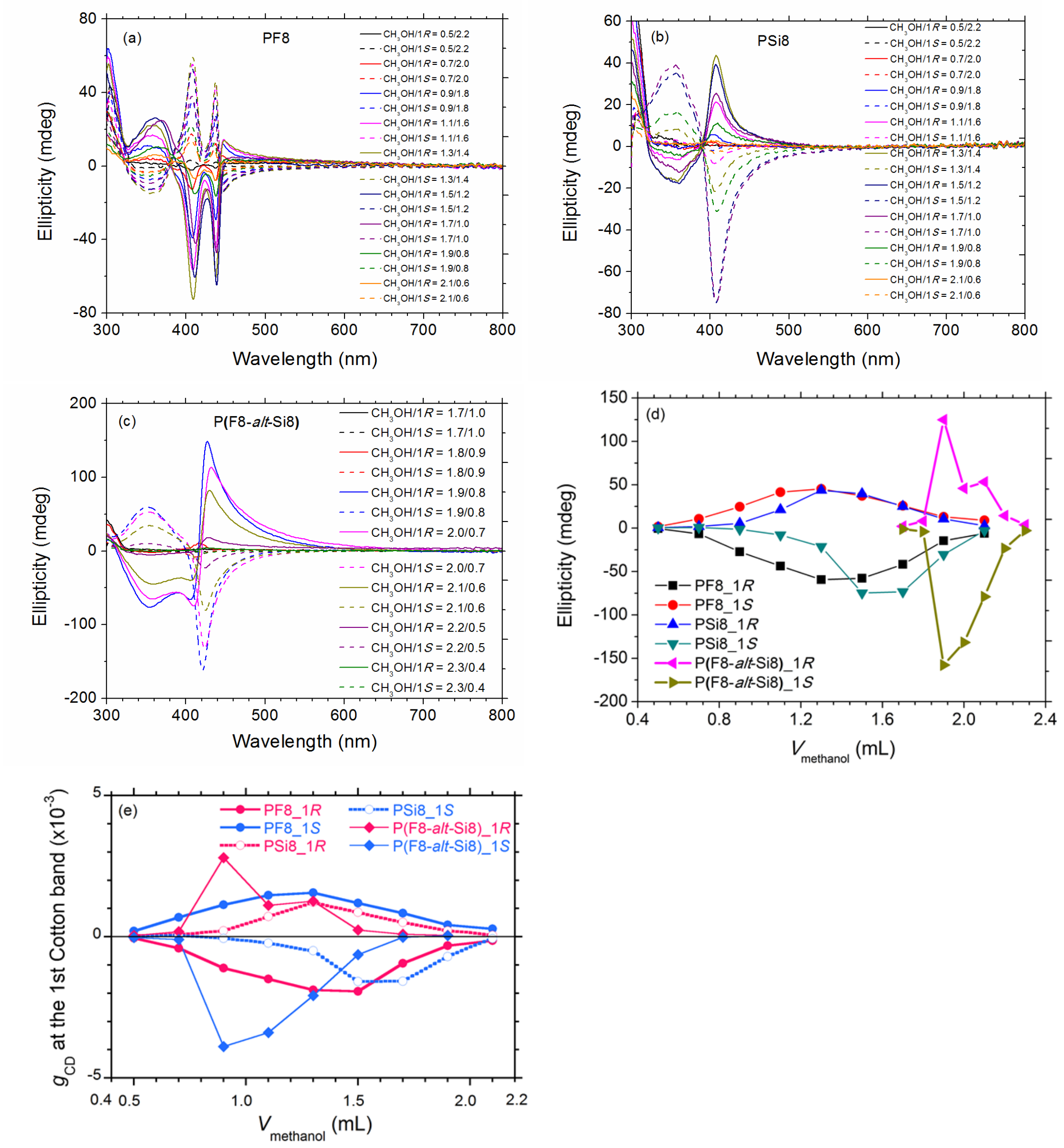

**Fig. S7** CD spectra at 25 °C of (a) **PF8**, (b) **PSi8**, and (c) **P(F8-*alt*-Si8)** aggregates and (d) the maximum CD values and (e) the $g_{CD}$ values of **PF8** (413 nm), **PSi8** (407 nm), and **P(F8-*alt*-Si8)** (423 nm) aggregates with different $CH_3OH$/**1*R*** or **1*S*** volume fractions (total volume is 3.0 mL, keeping $CHCl_3$ constant at 0.3 mL). The data in Figs. S7d and S7e were taken from Figs. S7a, S7b and S7c.The concentrations of the polymers are the same as those in Fig. 1a.

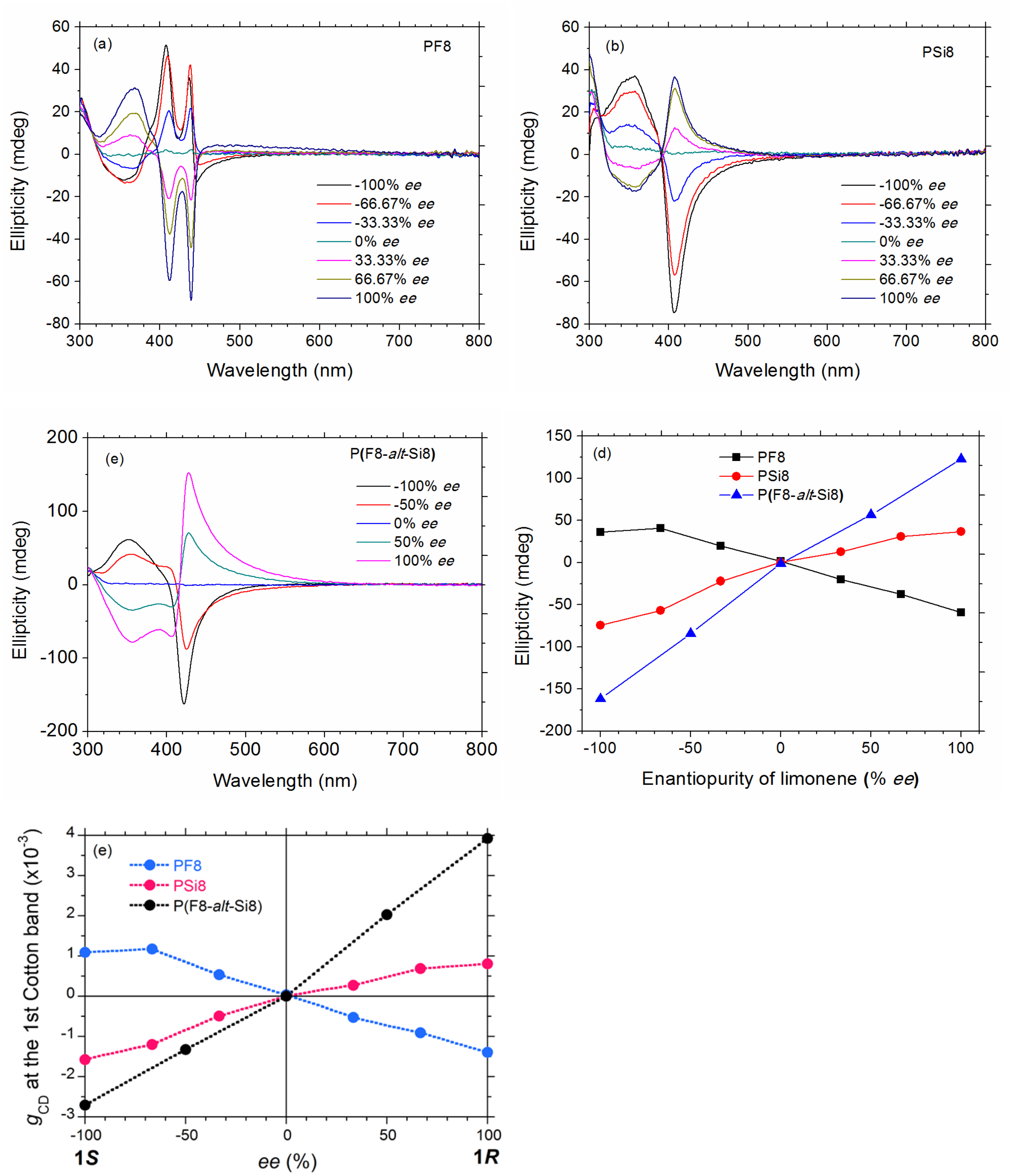

**Fig. S8** CD spectra at 25 °C of (a) **PF8**, (b) **PSi8**, and (c) **P(F8-*alt*-Si8)** aggregates. (d) The maximum CD values. (e) The $g_{\mathrm{CD}}$ values of **PF8** (413 nm), **PSi8** (407 nm), and **P(F8-*alt*-Si8)** (423 nm) aggregates in mixed tersolvents with different **1*R***/**1*S*** enantiopurities. The data in Figs. S8d and S8e were taken from Figs. S8a, S8b and S8c. $CHCl_3$/(**1*R***+**1*S***)/$CH_3OH$ = 0.3/1.2/1.5 (v/v/v) for **PF8** and **PSi8**, $CHCl_3$/(**1*R***+**1*S***)/$CH_3OH$ = 0.3/0.8/1.9 (v/v/v) for **P(F8-*alt*-Si8)**. The concentrations of the polymers are the same as those in Fig. 1a.

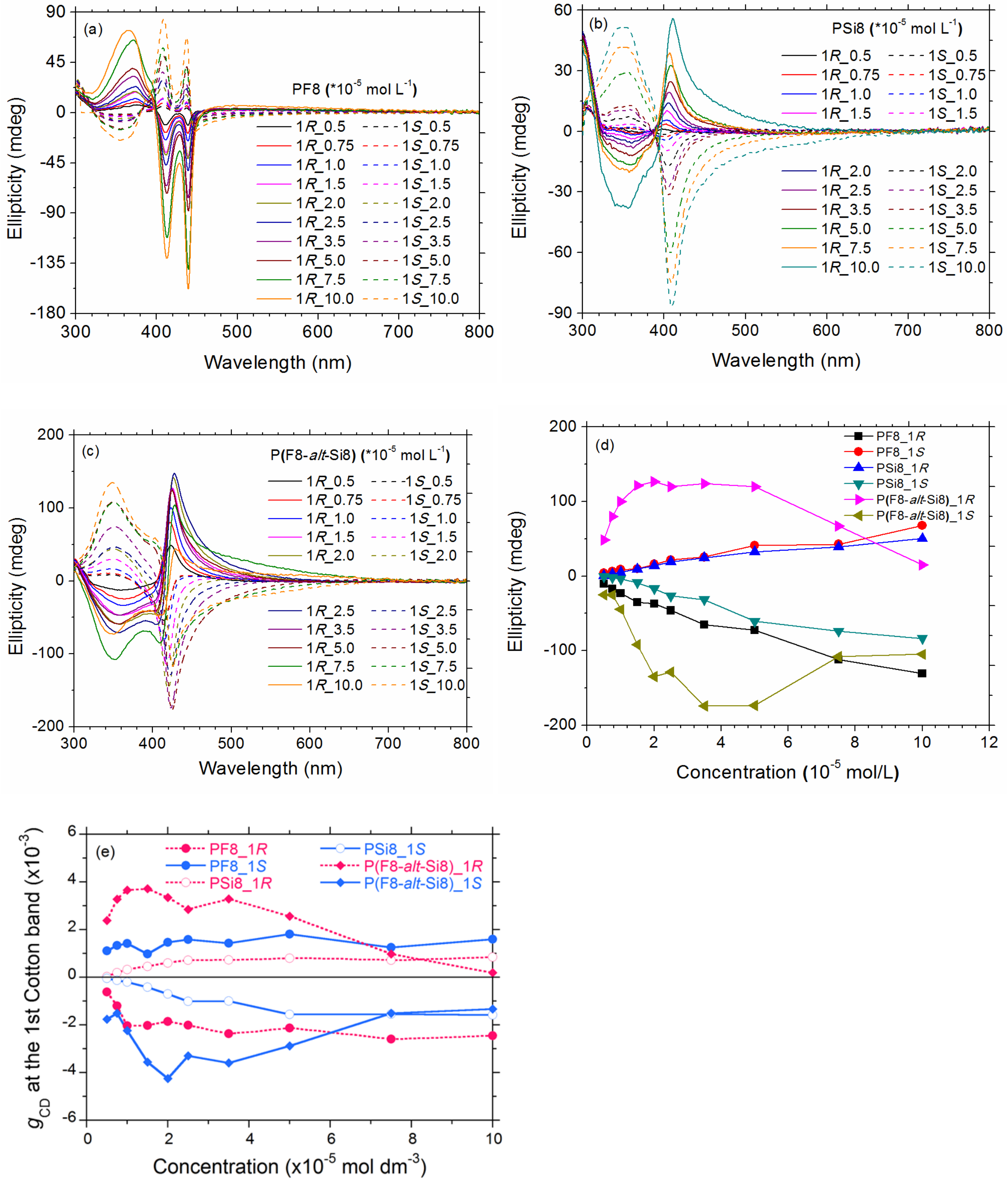

**Fig. S9** CD spectra at 25 °C of (a) **PF8**, (b) **PSi8**, and (c) **P(F8-*alt*-Si8)** aggregates. (d) The maximum CD values. (e) The $g_{CD}$ values of **PF8** (413 nm), **PSi8** (407 nm), and **P(F8-*alt*-Si8)** (423 nm) aggregates in mixed tersolvents at different concentrations of the polymers. The data in Figs. S9d and S9e were taken from Figs. S9a, S9b and S9c. $CHCl_3$/(**1*R*** or **1*S***)/$CH_3OH$ = 0.3/1.2/1.5 (v/v/v) for **PF8** and **PSi8**, $CHCl_3$/(**1*R*** or **1*S***) /$CH_3OH$ = 0.3/0.8/1.9 (v/v/v) for **P(F8-*alt*-Si8)**.

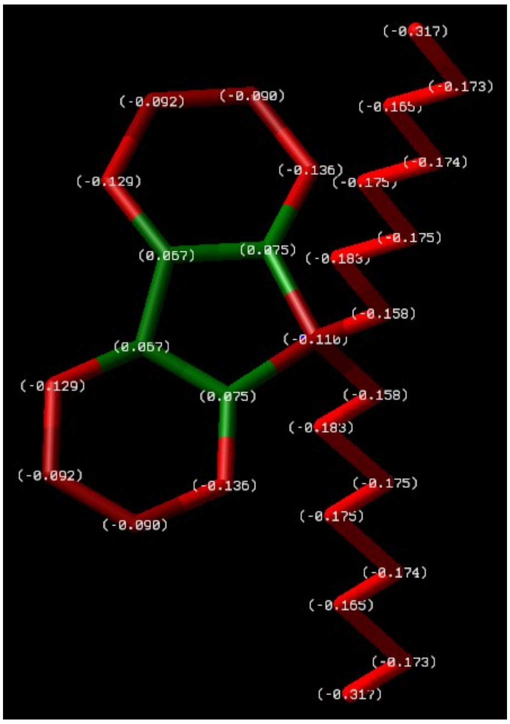

**F8** (ground state)

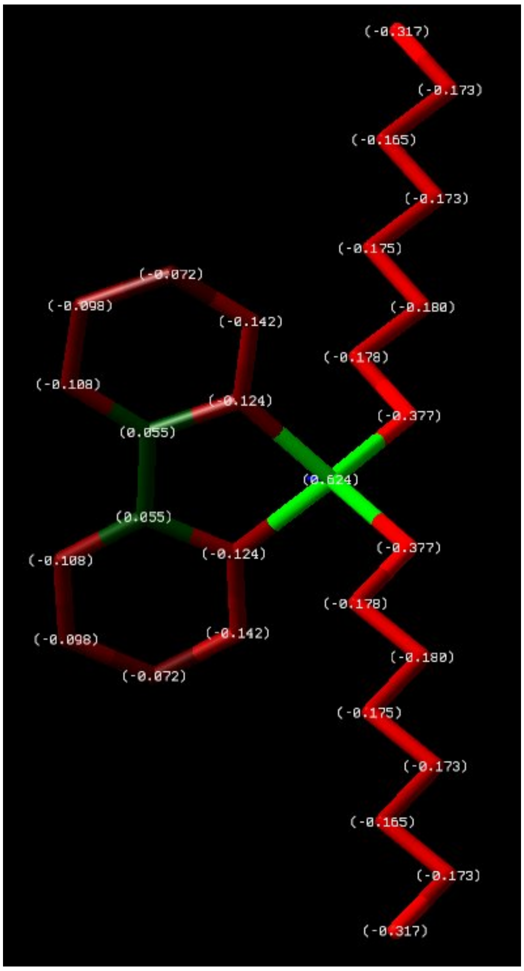

**Si8** (ground state)

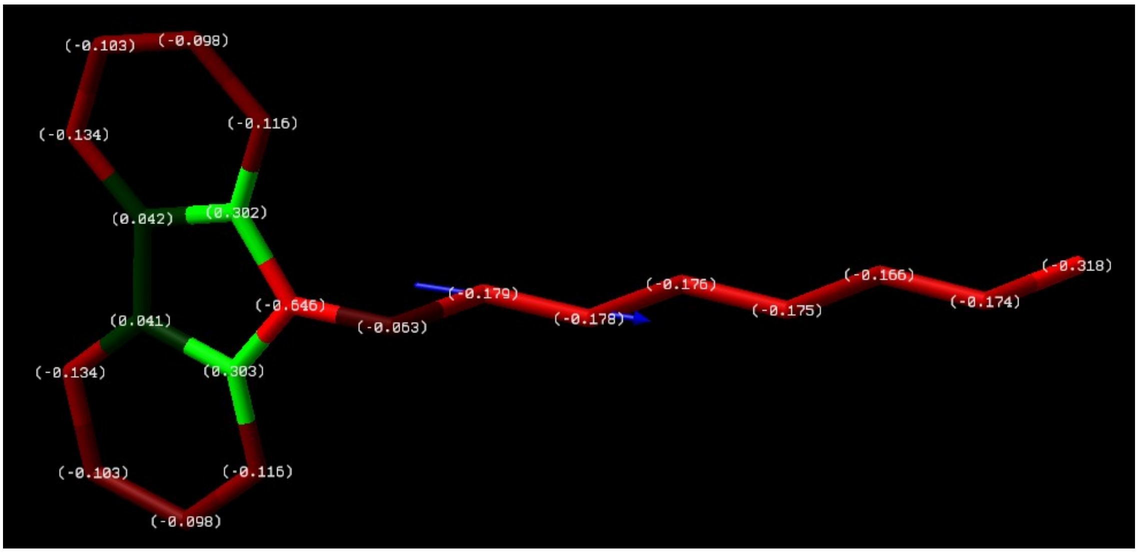

**Cz8** (ground state)

**Fig. S10a** Mulliken charges, dipole moment and its direction of **F8**, **Si8** and **Cz8** obtained with DFT calculation (B3LYP/6-31G(d,p)).

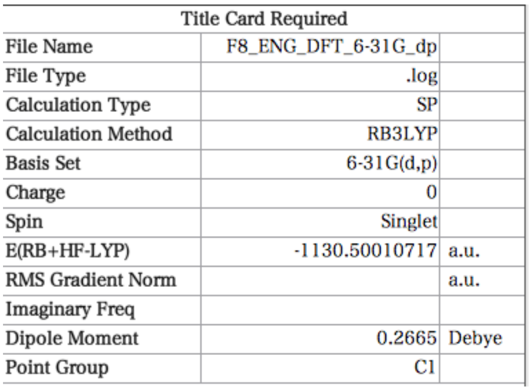

| Title Card Required | | |
|---|---|---|
| File Name | F8_ENG_DFT_6-31G_dp | |
| File Type | .log | |
| Calculation Type | SP | |
| Calculation Method | RB3LYP | |
| Basis Set | 6-31G(d,p) | |
| Charge | 0 | |
| Spin | Singlet | |
| E(RB+HF-LYP) | -1130.50010717 | a.u. |
| RMS Gradient Norm | | a.u. |
| Imaginary Freq | | |
| Dipole Moment | 0.2665 | Debye |
| Point Group | C1 | |

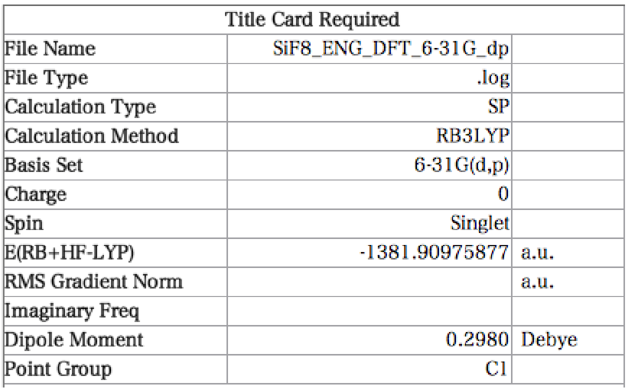

| Title Card Required | | |
|---|---|---|
| File Name | SiF8_ENG_DFT_6-31G_dp | |
| File Type | .log | |
| Calculation Type | SP | |
| Calculation Method | RB3LYP | |
| Basis Set | 6-31G(d,p) | |
| Charge | 0 | |
| Spin | Singlet | |
| E(RB+HF-LYP) | -1381.90975877 | a.u. |
| RMS Gradient Norm | | a.u. |
| Imaginary Freq | | |
| Dipole Moment | 0.2980 | Debye |
| Point Group | C1 | |

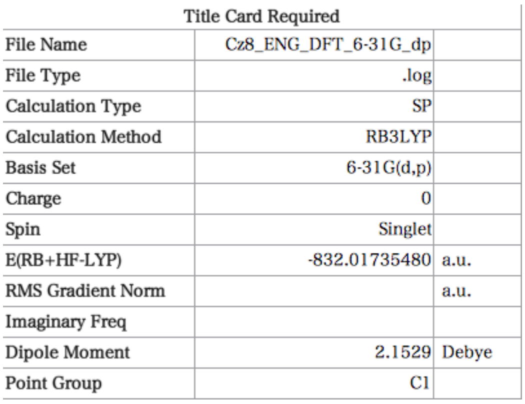

| Title Card Required | | |
|---|---|---|
| File Name | Cz8_ENG_DFT_6-31G_dp | |
| File Type | .log | |
| Calculation Type | SP | |
| Calculation Method | RB3LYP | |
| Basis Set | 6-31G(d,p) | |
| Charge | 0 | |
| Spin | Singlet | |
| E(RB+HF-LYP) | -832.01735480 | a.u. |
| RMS Gradient Norm | | a.u. |
| Imaginary Freq | | |
| Dipole Moment | 2.1529 | Debye |
| Point Group | C1 | |

**Fig. S10b** Mulliken charges, dipole moment and its direction of **F8**, **Si8** and **Cz8** in the ground state obtained with DFT calculation (B3LYP/6-31G(d,p) level).

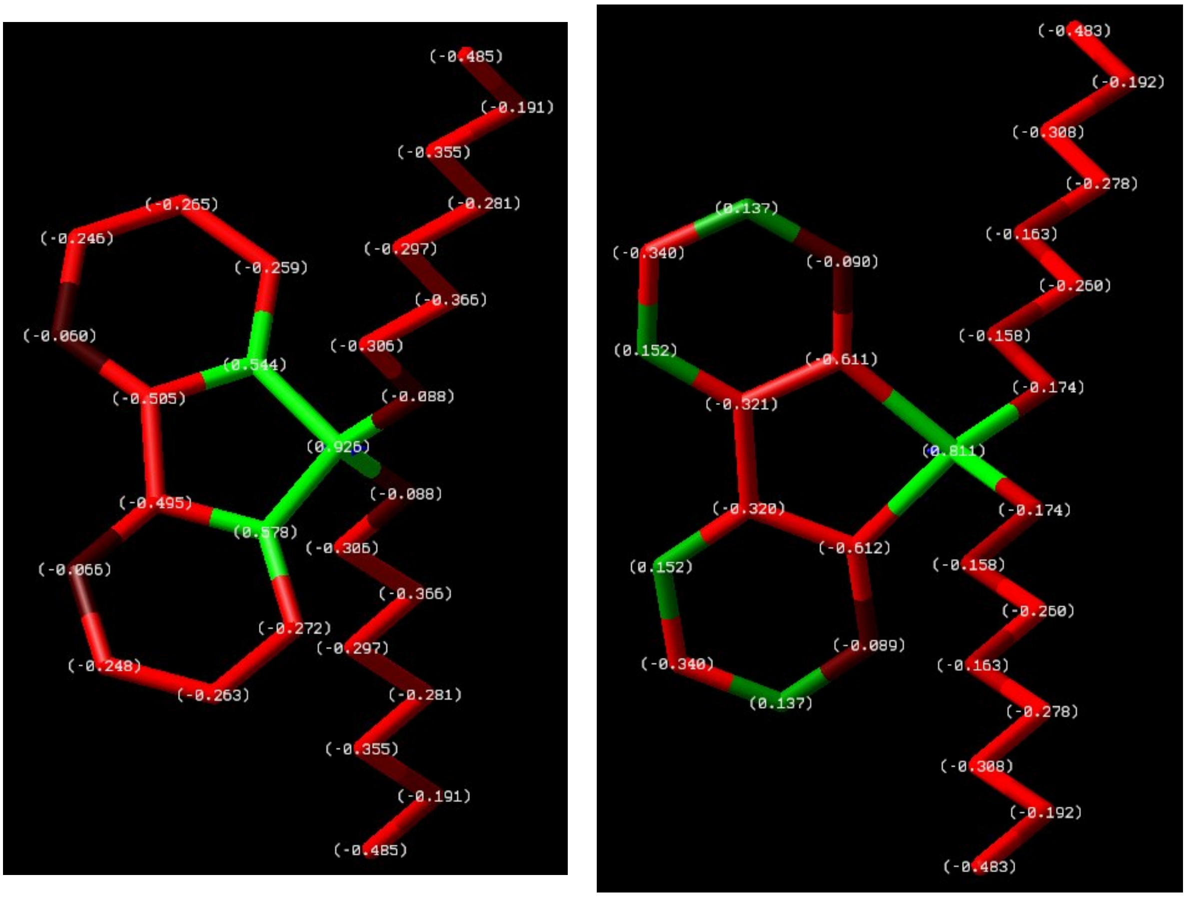

**F8** (excited state)

**Si8** (excited state)

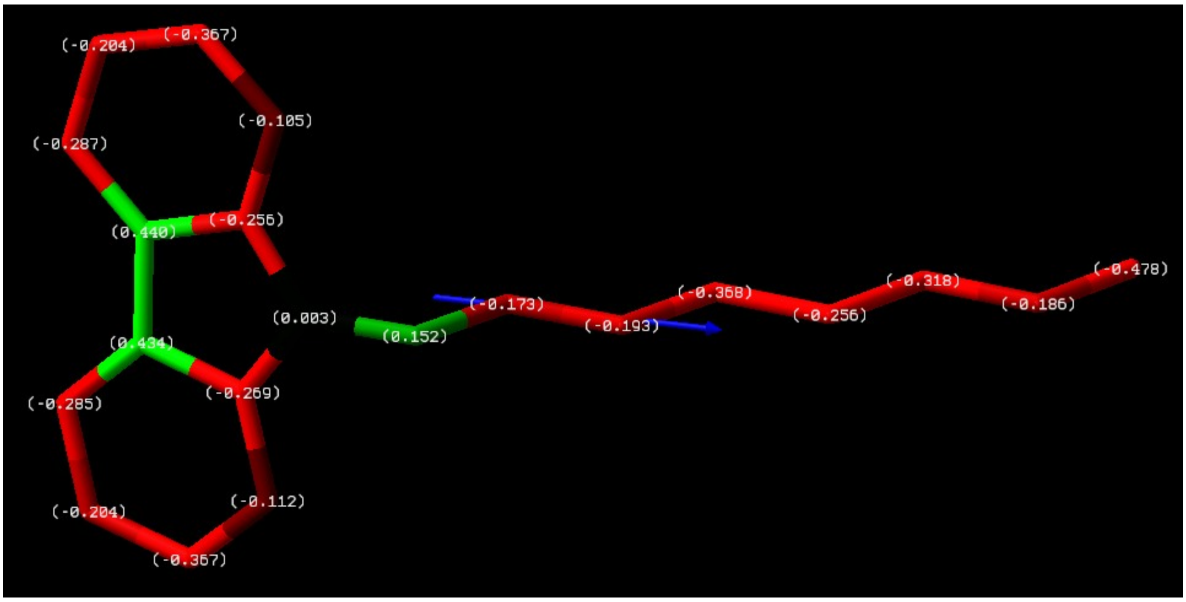

**Cz8** (excited state)

**Fig. S11a** Mulliken charges, dipole moment, and its direction of **F8**, **Si8** and **Cz8** in the excited state obtained with CIS calculation (6-31G(d,p) level).

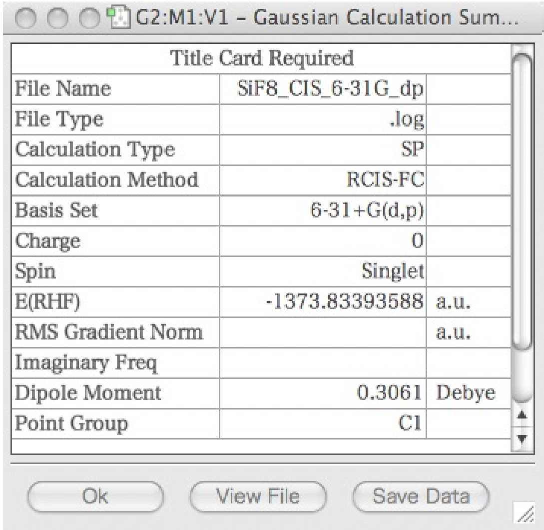

| Title Card Required | | |
|---|---|---|
| File Name | SiF8_CIS_6-31G_dp | |
| File Type | .log | |
| Calculation Type | SP | |
| Calculation Method | RCIS-FC | |
| Basis Set | 6-31+G(d,p) | |
| Charge | 0 | |
| Spin | Singlet | |
| E(RHF) | -1373.83393588 | a.u. |
| RMS Gradient Norm | | a.u. |
| Imaginary Freq | | |
| Dipole Moment | 0.3061 | Debye |
| Point Group | C1 | |

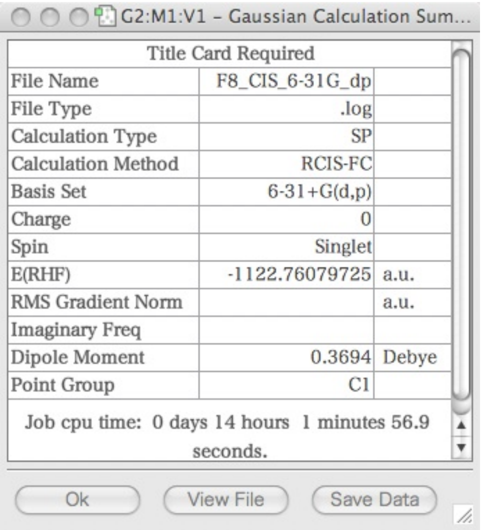

| Title Card Required | | |
|---|---|---|
| File Name | F8_CIS_6-31G_dp | |
| File Type | .log | |
| Calculation Type | SP | |
| Calculation Method | RCIS-FC | |
| Basis Set | 6-31+G(d,p) | |
| Charge | 0 | |
| Spin | Singlet | |
| E(RHF) | -1122.76079725 | a.u. |
| RMS Gradient Norm | | a.u. |
| Imaginary Freq | | |
| Dipole Moment | 0.3694 | Debye |
| Point Group | C1 | |

Job cpu time: 0 days 14 hours 1 minutes 56.9 seconds.

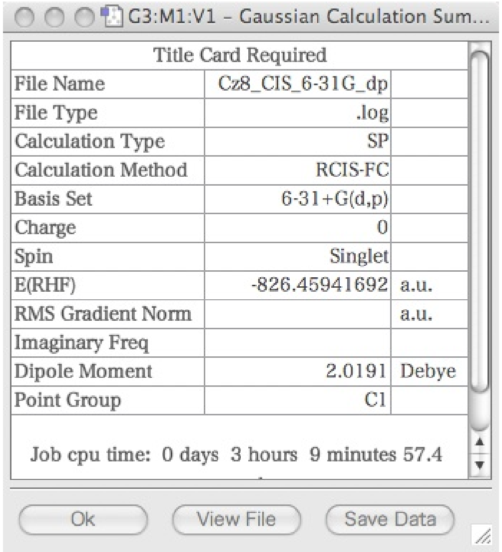

| Title Card Required | | |
|---|---|---|
| File Name | Cz8_CIS_6-31G_dp | |
| File Type | .log | |
| Calculation Type | SP | |
| Calculation Method | RCIS-FC | |
| Basis Set | 6-31+G(d,p) | |
| Charge | 0 | |
| Spin | Singlet | |
| E(RHF) | -826.45941692 | a.u. |
| RMS Gradient Norm | | a.u. |
| Imaginary Freq | | |
| Dipole Moment | 2.0191 | Debye |
| Point Group | C1 | |

Job cpu time: 0 days 3 hours 9 minutes 57.4

**Fig. S11b** Mulliken charges, dipole moment and its direction of **F8**, **Si8** and **Cz8** in the excited state obtained with CIS calculation (6-31G(d,p) level).

**Table S2**. Relative energy and dipole moment of three equatorial conformers of **1*R***.

| | Relative energy (kJ mol$^{-1}$) | Dipole moment (Debye) | Dipole direction | 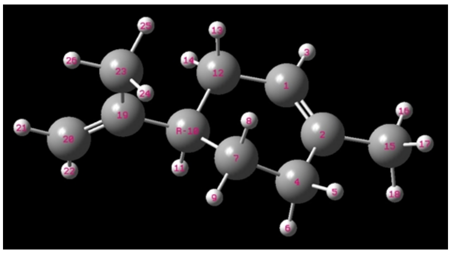 |
|---|---|---|---|---|
| EQ1 | 0.00 (0.00)¶ | 0.56 | from front to back | |
| EQ2 | 0.92 (0.69)¶ | 0.46 | from back to front | |
| EQ3 | 5.03 (1.71)¶ | 0.55 | from back to front. | |

¶ Data with B3LYP/cc-pVDZ level are taken from ref.8a in main text.

**Table S3.** Mulliken charges of ten carbon atoms from EQ1, EQ2, and EQ3 of **1*R***.

| | Carbon numbers | | | | | | | | | |
|---|---|---|---|---|---|---|---|---|---|---|
| | C1 | C2 | C3 | C4 | C5 | C6 | C7 | C8 | C9 | C10 |
| EQ1 | 0.13 | -0.12 | -0.20 | -0.12 | -0.19 | -0.23 | -0.37 | 0.18 | -0.30 | -0.37 |
| EQ2 | 0.13 | -0.12 | -0.20 | -0.11 | -0.19 | -0.23 | -0.37 | 0.16 | -0.29 | 0.37 |
| EQ3 | 0.13 | -0.13 | -0.19 | -0.12 | -0.17 | -0.23 | -0.37 | 0.17 | -0.29 | -0.37 |

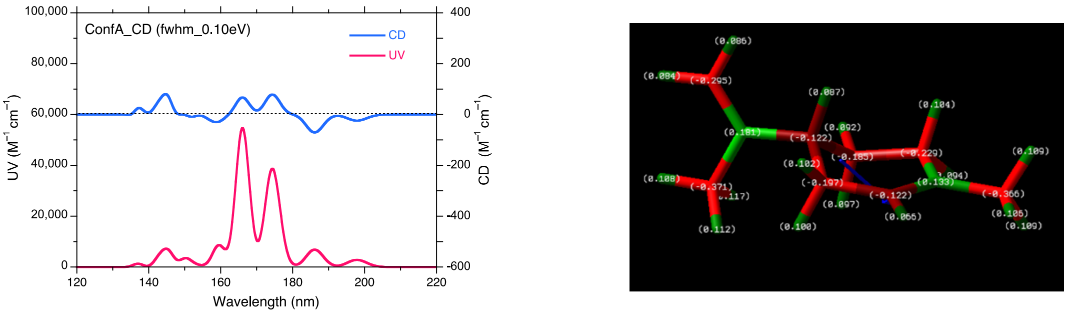

EQ1 (calculated UV/CD spectra and molecular shape)

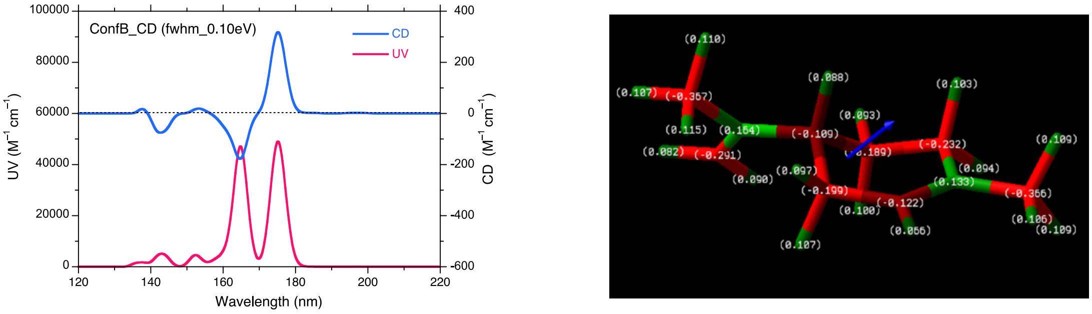

EQ2 (calculated UV/CD spectra and molecular shape)

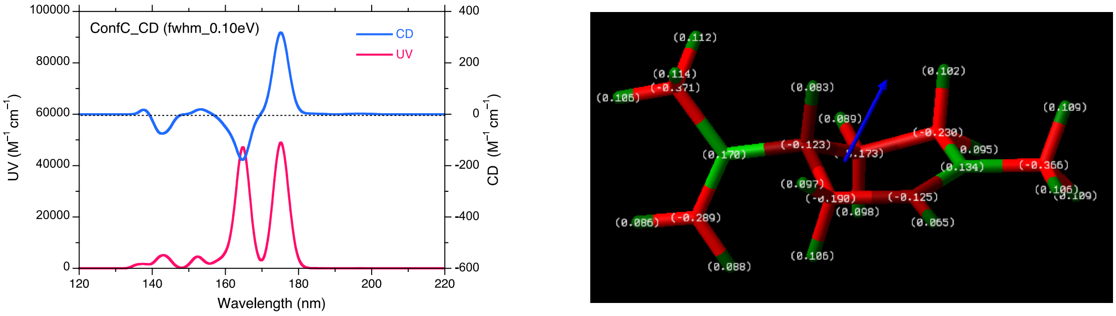

EQ3 (calculated UV/CD spectra and molecular shape)

**Fig. S12** (Top) Carbon and proton numbers of **1*R*** (EQ1). (Left column) Simulated CD and UV spectra of three equatorial **1*R*** rotamers (EQ1, EQ2, and EQ3) obtained with TD-DFT calculation (B3LYP/6-31G(d,p) level, with *fwhm* of 0.1 eV). (Right column) Mulliken charges, dipole moment, and dipole direction of EQ1, EQ2, and EQ3 by TD-DFT (B3LYP/6-31G(d,p) level).

*Mulliken charges and dipole moments of three stable **1R** conformers.* Our calculation showed that the three isomers, named EQ1, EQ2, and EQ3, have relative stability of 0.00, 0.92, 5.03 kJ mol$^{-1}$, respectively, as presented in Table S2. Among the three isomers, EQ3 is considerably stable using semi-empirical PM6 with PCM (solvent = methanol) for model trimers of **PF8** and **PSi8** supported a switching in preferential helicity when the same limonene chirality is applied and may exist as minor fraction in fluid solution. Because any polar atoms in **1*R*** are absent, EQ1, EQ2, and EQ3 have small dipole moments as 0.56, 0.46, and 0.55 Debye, respectively. Also, Mulliken charges of ten carbon atoms in EQ1, EQ2, and EQ3 have no significant difference, as given in Table S3. However, it is noted that dipole *direction* of EQ1 is the opposite to that of EQ2 and EQ3, as given in Table S2 and Fig. S12, right column. The opposite direction may be related to the chiroptical inversion of **PF8** and **PSi8**. For example, optically active **PF8** aggregates can be induced by **1*R*** EQ2, while optically active **PSi8** aggregates are induced by **1*R*** EQ1 or vice versa.